AGU ADVANCING EARTH AND SPACE SCIENCE

Water Resources Research

RESEARCH ARTICLE
10.1029/2021WR031181

Watershed-Geochemical Model to Simulate Dissolved and Particulate ^{137}Cs Discharge From a Forested Catchment

Kazuyuki Sakuma[1], Seiji Hayashi[2], Kazuya Yoshimura[1], Hiroshi Kurikami[1], Alex Malins[3], Hironori Funaki[1], Hideki Tsuji[2], Takamaru Kobayashi[4], Akihiro Kitamura[1], and Kazuki Iijima[1]

[1]Sector of Fukushima Research and Development, Japan Atomic Energy Agency, Fukushima, Japan, [2]Fukushima Branch, National Institute of Environmental Studies, Fukushima, Japan, [3]Center for Computational Science & e-Systems, Japan Atomic Energy Agency, Chiba, Japan, [4]Geosphere Environmental Technology Corporation, Tokyo, Japan

Key Points:

- A coupled watershed-geochemical model is introduced for simulating dissolved contaminant transport from forests into river water
- The model reproduced dissolved ^{137}Cs concentration trends in Ohta River, Fukushima Prefecture, in base- and stormflow periods
- The results supported the theory that the organic layer is an important contamination source for river water

Supporting Information:

Supporting Information may be found in the online version of this article.

Correspondence to:

K. Sakuma,
sakuma.kazuyuki@jaea.go.jp

Citation:

Sakuma, K., Hayashi, S., Yoshimura, K., Kurikami, H., Malins, A., Funaki, H., et al. (2022). Watershed-geochemical model to simulate dissolved and particulate ^{137}Cs discharge from a forested catchment. *Water Resources Research*, *58*, e2021WR031181. https://doi.org/10.1029/2021WR031181

Received 7 SEP 2021
Accepted 28 JUL 2022

Abstract Measurements in forest catchments in Fukushima Prefecture indicate that cesium-137 (^{137}Cs) leaching from forest litter affects dissolved ^{137}Cs levels in river water. Existing simulations have been unsuccessful in reproducing this phenomenon due to mechanistic limitations in the models connecting the forest ecosystem and the river system. This paper introduces a new coupled watershed-geochemical model to address this. We connected a forest ecosystem compartment model to the 3D watershed model General-purpose Terrestrial Fluid-Flow Simulator to describe ^{137}Cs transfer between forests and the river system. The compartment model included nonleachable and leachable ^{137}Cs sites in the organic layer. The latter sites model how leachable ^{137}Cs stocks increase with ambient temperature owing to decomposing organic matter. The model was tested by simulating dissolved and particulate ^{137}Cs discharges from a forested catchment upstream of the Ohta River, Fukushima Prefecture. The results for dissolved ^{137}Cs concentrations in river water for 1 January 2014, to 31 December 2015, correlated well with catchment measurements. The simulations reproduced dissolved ^{137}Cs concentration peaks that occurred during three typhoon events and the seasonal variations under baseflow conditions. The results support the theory that leaching from the organic layer in forests is a primary factor affecting river water dissolved ^{137}Cs concentrations. The wider contribution of this study is it introduces a coupled watershed-geochemical model, applicable not only for evaluating the dynamics of ^{137}Cs, but also those of other substances that adsorb onto sediments and soil particles, and leach from forest organic matter.

Plain Language Summary Cesium-137 (^{137}Cs) derived from the Fukushima Daiichi Nuclear Power Plant is a critical radioisotope remaining from the fallout owing to its high activity, long half-life (30.1 y), and potential impacts on humans and ecosystems. Approximately 70% of all land in Fukushima Prefecture is covered with forests, where ^{137}Cs is predominantly present. The behavior of dissolved ^{137}Cs in the environment must be investigated because this form of ^{137}Cs is readily absorbed by living beings. Researchers have reported that dissolved ^{137}Cs concentrations in river water under baseflow conditions vary seasonally and rise during storms, indicating that leaching from organic matter in forests is a dissolved ^{137}Cs source. We developed a new simulation model for the dynamics of ^{137}Cs between the forest ecosystem and the river system. The simulations reproduced the dissolved ^{137}Cs concentration peaks that occurred during previous typhoons and the seasonal variations that occurred under baseflow conditions. Therefore, the model's results support the theory that leaching from the organic layer in forests is a primary factor affecting dissolved ^{137}Cs concentrations in river water. The model introduced here can not only be used for simulating ^{137}Cs, but also has wider applicability for simulating the transport mechanisms of other contaminants through forest watersheds.

1. Introduction

The Fukushima Daiichi Nuclear Power Plant (FDNPP) accident occurred owing to the earthquake and tsunami on 11 March 2011, and caused environmental radioisotope pollution in terrestrial areas (Ministry of Education, Culture, Sports, Science and Technology, 2011). Cesium-137 (^{137}Cs) is a critical radioisotope remaining from the fallout owing to its high activity, long half-life (30.1 y), and potential impacts on humans and ecosystems.

Approximately 70% of all land in Fukushima Prefecture is forest (Ministry of Agricultural, Forestry, and Fisheries, 2012), and ^{137}Cs is deposited predominantly in forest areas (Nakanishi et al., 2021). The affected forests have not been decontaminated (Ministry of the Environment, 2012). Around 65%–91% of the ^{137}Cs in the forests was

present within the top 5 cm of the surface soil in 2015 (Imamura et al., 2017). Understanding how ^{137}Cs migrates from the forest ecosystem to the river system is essential for assessing water resources in contaminated regions after the nuclear accident.

Watershed modeling is frequently used to achieve these aims. Several distributed hydrological models have been developed for catchment-scale simulations globally, for example, InHM (Jones et al., 2008), ParFlow (Kollet and Maxwell, 2006; Siirila-Woodburn et al., 2018), WEPP (Laflen et al., 1991), HydroGeoSphere (Goderniaux et al., 2009), SHETRAN (Ewen et al., 2000), Mike-SHE (Graham & Butts, 2005), and SWAT (Malagó et al., 2017; Santhi et al., 2006). Because some radionuclides tend to be adsorbed on soil particles, water circulation simulations must consider radionuclide sediment transport and chemical reactions. However, these existing codes do not have the functionality for simulating radionuclides transported by waterflow, sediment redistribution, and chemical reactions. Some watershed-scale models for radiocesium transport due to waterflow and sediment redistribution were developed after the FDNPP accident (Kinouchi et al., 2015; Mori et al., 2015; Sakuma et al., 2017;Sakuma, Malim, et al. 2018; Sakhuma, Tsuji et al. 2018; Wei et al., 2017). Other simulation models for radiocesium transport in rivers and reservoirs, but not on the watershed-scale, were developed after the Chernobyl and FDNPP accidents, for example, TODAM (Kurikami et al., 2014; Onishi & Yokuda, 2013), RIVTOX (Zheleznyak et al., 1997), THREETOX (Zheleznyak, 1997), FLESCOT (Kurikami et al., 2016; Onishi et al., 1993), and 3D-Sea-SPEC (Yamada et al., 2020). Most codes model the absorption and desorption between the dissolved and bound states using distribution coefficients (K_d) because they focus on particulate radiocesium behavior once it is present in the water body.

Researchers in Fukushima have reported that dissolved ^{137}Cs concentrations in river water under baseflow conditions have a seasonal variation correlated with the temperature (high in summer and low in winter) (Muto et al., 2017; Nakanishi & Sakuma, 2019; Tsuji et al., 2016). Moreover, dissolved ^{137}Cs concentrations in river water sampled in the same season are higher under stormflow conditions than baseflow conditions (Iwagami et al., 2017; Shinomiya et al., 2014; Tsuji et al., 2016; Yoshikawa et al., 2014). Furthermore, the ^{137}Cs activity of forest litter in the riparian zone was approximately 10 times higher than that of accumulated forest litter submerged in stream riverbeds (Murakami et al., 2014; Sakai et al., 2016). Leaching tests indicate that contaminated litter in headwaters relates to elevated ^{137}Cs (Sakakibara et al., 2021).

On the modeling side, Sakuma, Tsuji, et al. (2018) revealed the limitations of using distribution coefficients (K_d) between particulate and dissolved ^{137}Cs for simulating dissolved ^{137}Cs concentrations in river water within forest catchments. Simulations could reproduce the mean dissolved ^{137}Cs concentration in river water under baseflow conditions. However, they were unsuccessful in reproducing the peaks in dissolved ^{137}Cs concentrations during storms and the seasonal variability observed under baseflow conditions. This discrepancy could be due to the inadequate modeling of ^{137}Cs leaching from organic matter. Experiments by Sakuma et al. (2021) showed that ^{137}Cs leaching rates from litter depend on ambient environmental parameters, such as temperature, indicating that the organic layer in forests is a source of dissolved ^{137}Cs in river water. The experimental evidence thus indicates that ^{137}Cs leaching from organic matter affects dissolved ^{137}Cs concentrations base- and stormflow conditions. However, a simulation model which captures this mechanism has yet to be presented.

The goal of this study was to develop a watershed model which captures mechanisms of both particulate-bound and dissolved ^{137}Cs exchange between forests and river systems. This is achieved by coupling a watershed and a geochemical forest compartment model and evaluating the seasonal and storm-related dynamics of ^{137}Cs leaching from forest matter and transferring them to river water. The model presented herein is evaluated by simulating dissolved and particulate-bound ^{137}Cs concentrations in river water in a forested catchment in Fukushima Prefecture and comparing it against field observations.

2. Materials and Methods

2.1. Site Description

The upstream Ohta River catchment (Figure 1) covers 21 km^2 and lies 24.4 km northwest of the FDNPP site in Fukushima Prefecture (Sakuma, Tsuji, et al., 2018; Tsuji et al., 2016). The mean ^{137}Cs inventory was approximately 1.9 MBq m^{-2} in July 2011, based on the third airborne monitoring survey (Ministry of Education, Culture, Sports, Science and Technology, 2011). The primary land use is forest, covering 99.2% of the catchment area (Ministry of the Environment, 2016). The main surface soil is haplic cambisols (National Agriculture and Food

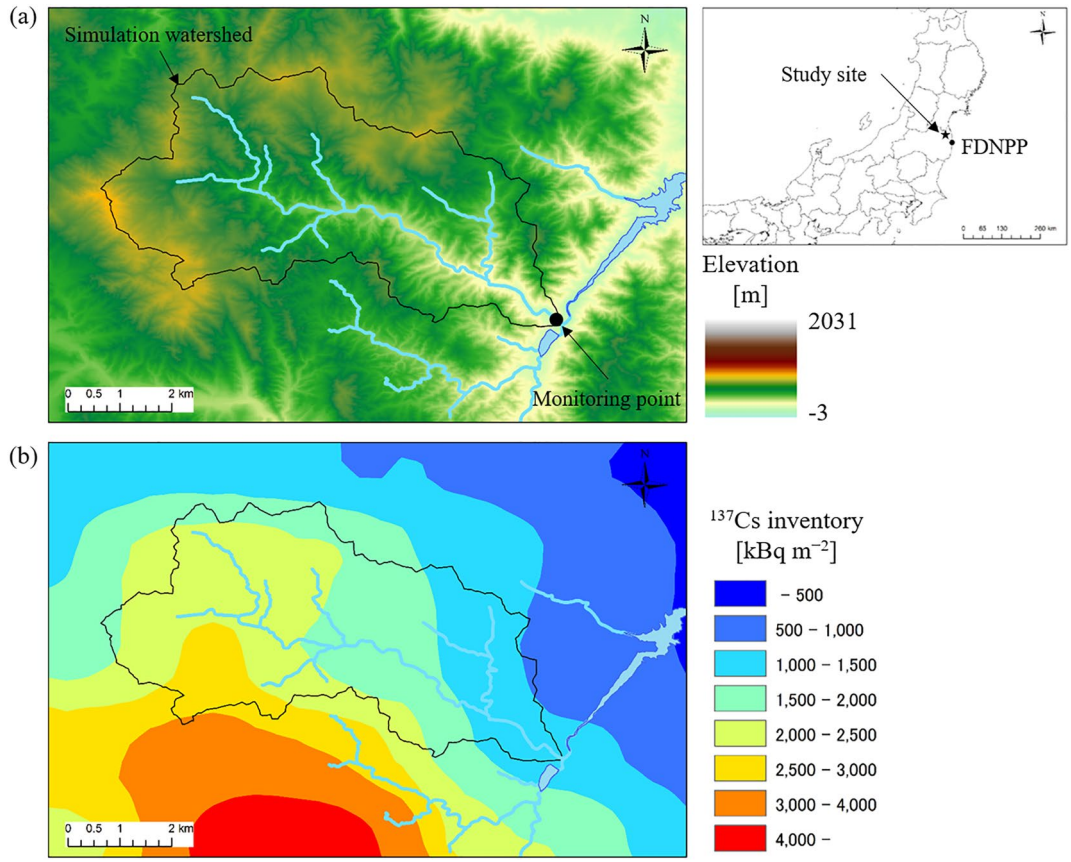

Figure 1. A map showing the upstream Ohta River catchment (enclosed by the black boundary line). (a) The topography and (b) ^{137}Cs inventory in July 2011.

Research Organization, 2021). The bedrock is primarily granite and diorite (National Institute of Advanced Science and Technology, 2016). The average annual precipitation and temperature between 1991 and 2020 at the Iitate weather station were 1,367 mm and 10.3°C, respectively (Japan Meteorological Agency, 2021). Furthermore, the average monthly precipitation at the same station was 190 and 45 mm, for August and December respectively (Japan Meteorological Agency, 2021); therefore, water discharge rates from this catchment are higher in summer than in winter. No decontamination activities have taken place in this catchment's forests. The catchment's river water drains to the Yokokawa dam reservoir in Minamisoma City, Fukushima Prefecture. Some reservoir water is extracted for industrial water use. The Yokokawa dam drains downstream toward agricultural land and urban areas.

2.2. Model Description

A combined watershed-geochemical model was developed by coupling the GETFLOWS watershed model (Mori et al., 2015; Sakuma et al., 2017; Sakuma, Malins, et al., 2018; Sakuma, Tsuji, et al., 2018; Tosaka et al., 1996) with a forest ecosystem compartment model. A brief explanation of the GETFLOWS model is as follows. Figure 2 (a) shows a diagram of the model. The code calculates surface waterflows, subsurface air and waterflows, soil detachment due to rainfall and sediment transport via soil erosion, and sediment transport within surface waterflows and redeposition. For surface waterflows, the diffusive wave approximation of the shallow water equations is assumed for river streams and hillslopes. These equations are solved using a fully implicit method for surface waterflows and subsurface air and waterflows. For waterflow soil erosion and deposition, the transport capacity model (Morgan et al., 1998) is applied to estimate the net soil erosion and deposition for each soil particle size. Also, the kinetic energy of raindrops is calculated for each land use to evaluate the detachment of soil particles by raindrops. Advection/diffusion equations of sediment transport considering these phenomena are solved.

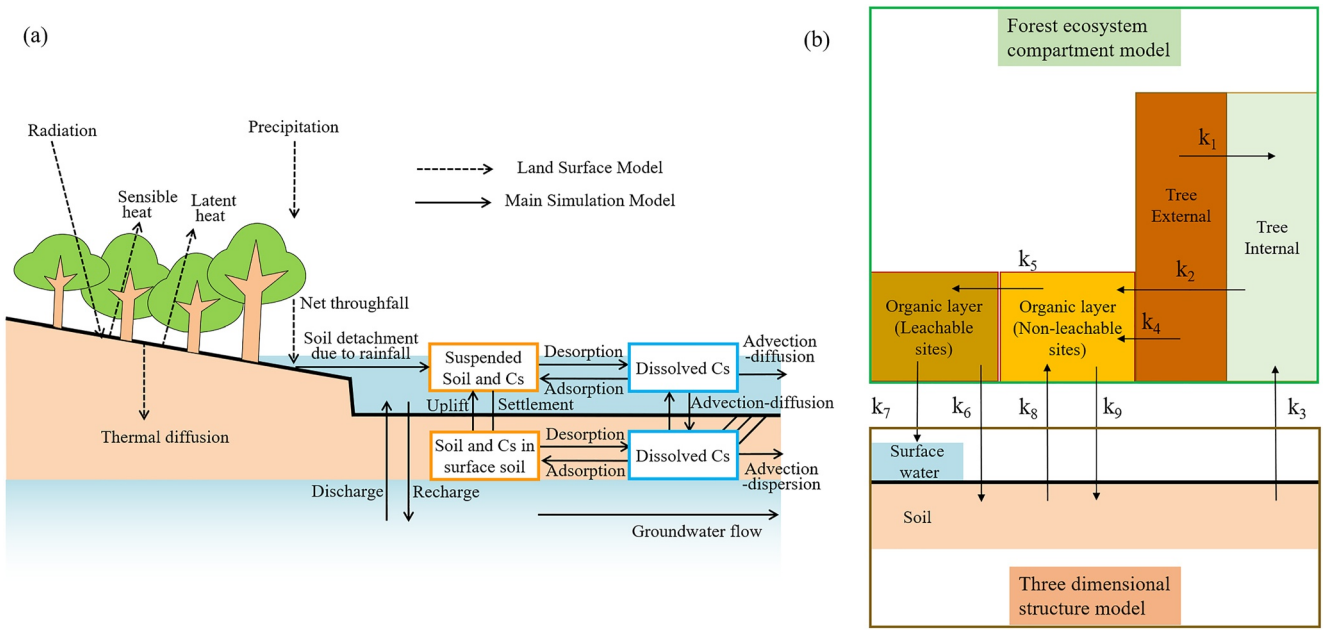

Figure 2. (a) A diagram of the GETFLOWS model (modified Figure 5 of Kitamura et al., 2016). (b) A diagram of the forest ecosystem compartment model coupled to GETFLOWS.

Cesium-137 transport is calculated for particulate and dissolved forms. The ^{137}Cs partitioning between particulate and dissolved phases was modeled with distribution coefficients (K_d) assuming equilibrium. Conservation laws for each mass were provided in Mori et al. (2015).

2.3. The Conservation Law for Dissolved ^{137}Cs Transport Is

$$-\nabla\cdot(M_w R_{cw})+\nabla\cdot D_{cw}\nabla(\rho_w R_{cw})-\rho_w q_w R_{cw}-\lambda\rho_w\varphi S_w R_{cw}+\rho_w R_{ss,i} m_i^{adsorp} + \rho_{ss,i}(1-\varphi)m_i^{adsorp}=\frac{\partial}{\partial t}(\rho_w\varphi S_w R_{cw}) \quad (1)$$

where M_w is the water mass flux (kg m^{-2} s^{-1}), R_{cw} is the mass fraction of dissolved ^{137}Cs in the water (kg kg^{-1}), and D_{cw} is the hydrodynamic dispersion coefficient (m^2 s^{-1}). ρ_w is the water density (kg m^{-3}), q_w is the volumetric flux of water sinks and sources (m^3 m^{-3} s^{-1}), λ is the decay constant of ^{137}Cs (s^{-1}), φ is the effective porosity (m^3 m^{-3}), and S_w is the saturation factor (m^3 m^{-3}). $R_{ss,i}$ is the mass fraction of suspended sediment particle grade i within the water (kg kg^{-1}), m_i^{adsorp} is the absorption/desorption rate of dissolved to/from particulate-bound ^{137}Cs (s^{-1}), $\rho_{ss,i}$ is the density of sediment grade i (kg m^{-3}), and t is the time (s).

The final two terms on the left-hand side of Equation 1 represent the ^{137}Cs transfer between the dissolved and particulate fractions. The first term applies to the surface layer cells, where adsorption/desorption can occur on suspended sediments within surface water. The second term applies to subsurface layers, where adsorption/desorption can occur on soil particles. That is, Equation 1 is valid for surface and subsurface water; however, the adsorption and desorption terms $\rho_w R_{ss,i} m_i^{adsorp}$ and $\rho_{ss,i}(1-\varphi)m_i^{adsorp}$ concern only surface and subsurface water, respectively. The absorption and desorption rates are provided by

$$m_{ss,i}^{adsorp}=a_i^{1,2}(K_{d,i}R_{cw}-R_{cs,i}) \quad (2)$$

where $a_i^{1,2}$ is the rate constant (s^{-1}), $K_{d,i}$ is the ^{137}Cs distribution coefficient between the dissolved and bound states (kg kg^{-1}), and $R_{cs,i}$ is the mass fraction of ^{137}Cs bound to the particulates (kg kg^{-1}).

Figure 2 (b) is a diagram of the forest ecosystem compartment model coupled with GETFLOWS. This model was based on the radionuclides in forest ecosystems 1 (RIFE1) model (Hashimoto et al., 2013; Shaw et al., 2005). The original RIFE1 model includes five compartments (tree external, tree internal, litter, organic soil, and mineral soil); however, the modified version we use has only three components (tree external, tree internal, and organic

layer). Referring to Ota et al. (2016), we divided the forest litter compartment (the organic layer) into leachable and non-leachable Cs sites. The organic and mineral soil compartments in the RIFE1 model could be excluded because they are equivalent to the top surface soil in the 3D hydrogeological structure model of GETFLOWS. The tree internal and organic layer (leachable and non-leachable Cs sites) compartments were coupled directly with the GETFLOWS model using each value at the same time-steps. Each grid cell of the 3D hydrogeological structure model with forest land use had a coupled forest compartment model (tree external, tree internal, leachable, and non-leachable site organic layer compartments). The conservation laws obeyed were

$$\frac{dI_1}{dt} = -k_1 I_1 - k_4 I_1 - \lambda I_1 \tag{3}$$

$$\frac{dI_2}{dt} = k_1 I_1 - k_2 I_2 + k_3[soil] - \lambda I_2 \tag{4}$$

$$\begin{aligned} \frac{dI_3}{dt} &= k_2 I_2 + k_4 I_1 - k_5 I_3 + k_8[soil] - k_9 I_3 - \lambda I_3, \text{ and} \\ \frac{dI_4}{dt} &= k_5 I_3 - k_6 I_4 - k_7 I_4 - \lambda I_4, \end{aligned} \tag{5}$$

$$\text{if the water depth is under the threshold water depth, then } k_7 = 0, \tag{6}$$

where I_1, I_2, I_3, and I_4 are the ^{137}Cs inventory of tree external, tree internal, non-leachable, and leachable site organic layer compartments (Bq m^{-2}), respectively. k_1 is the kinetic rate (s^{-1}) for transfers from tree external to tree internal, k_2 is the kinetic rate (s^{-1}) for transfers from tree internal to non-leachable site organic layer, k_3 is the kinetic rate (s^{-1}) for the transfers from soil to tree internal, k_4 is the kinetic rate (s^{-1}) for transfers from tree external to non-leachable site organic layer, k_5 is the kinetic rate (s^{-1}) for the transfers from non-leachable site organic layer to leachable site organic layer, k_6 is the kinetic rate (s^{-1}) for the transfers from leachable site organic layer to the soil, k_7 is the kinetic rate (s^{-1}) for the transfers from leachable site organic layer to surface water, k_8 is the kinetic rate (s^{-1}) for the transfers from soil to non-leachable site organic layer, and k_9 is the kinetic rate (s^{-1}) for the transfers from non-leachable site organic layer to soil. [*soil*] is the ^{137}Cs inventory of the top layer of the 3D hydrogeological structure model (Bq m^{-2}), and water depth (m) is the water depth in each surface water layer grid cell in the structure model.

The ^{137}Cs transfer from the non-leachable Cs site to the leachable Cs site in the organic layer (k_5) depends on the bulk temperature in each grid cell, based on the results of a litterbag experiment for the weight loss rate of several forest litter types (Kawahara, 1985). The equation is

$$k_5 = A \times \exp(B + CT) \tag{7}$$

where A (s^{-1}), B (−), and C (°C^{-1}) are constants, and T is the temperature of the grid cell (°C).

The transfer from the leachable site organic layer to soil (k_6) depends only on time. The model does not consider the effect of wash-off due to precipitation.

Figure 3 (a) shows a 3D hydrogeological structure model of the study area. Further information about this model was provided in Sakuma, Tsuji, et al. (2018). The model was developed for the upstream Ohta River catchment (Figure 1) by combining surface topography data from the Geospatial Information Authority of Japan (2012) and subsurface geology data from the Geological survey of Geospatial Information Authority of Japan (2012). The land surface was segregated into 13,104 cells with sides averaging 40 m in width and breadth. The model comprised one air layer, one surface layer, and 20 subsurface layers (total = 288,288 grid blocks).

2.4. Parameters and Input Data

Tables S1–S6 show the various input parameters used in this simulation for water and sediment transport. These parameters were identical to those used in Sakuma, Tsuji, et al. (2018).

The ^{137}Cs inventory distribution used for the initial simulation condition was estimated based on the eighth airborne monitoring survey conducted November 2–19, 2013, and reported by the Ministry of Education, Culture, Sports, Science and Technology (Nuclear Regulation Authority, 2013). Details of obtaining the ^{137}Cs inventory

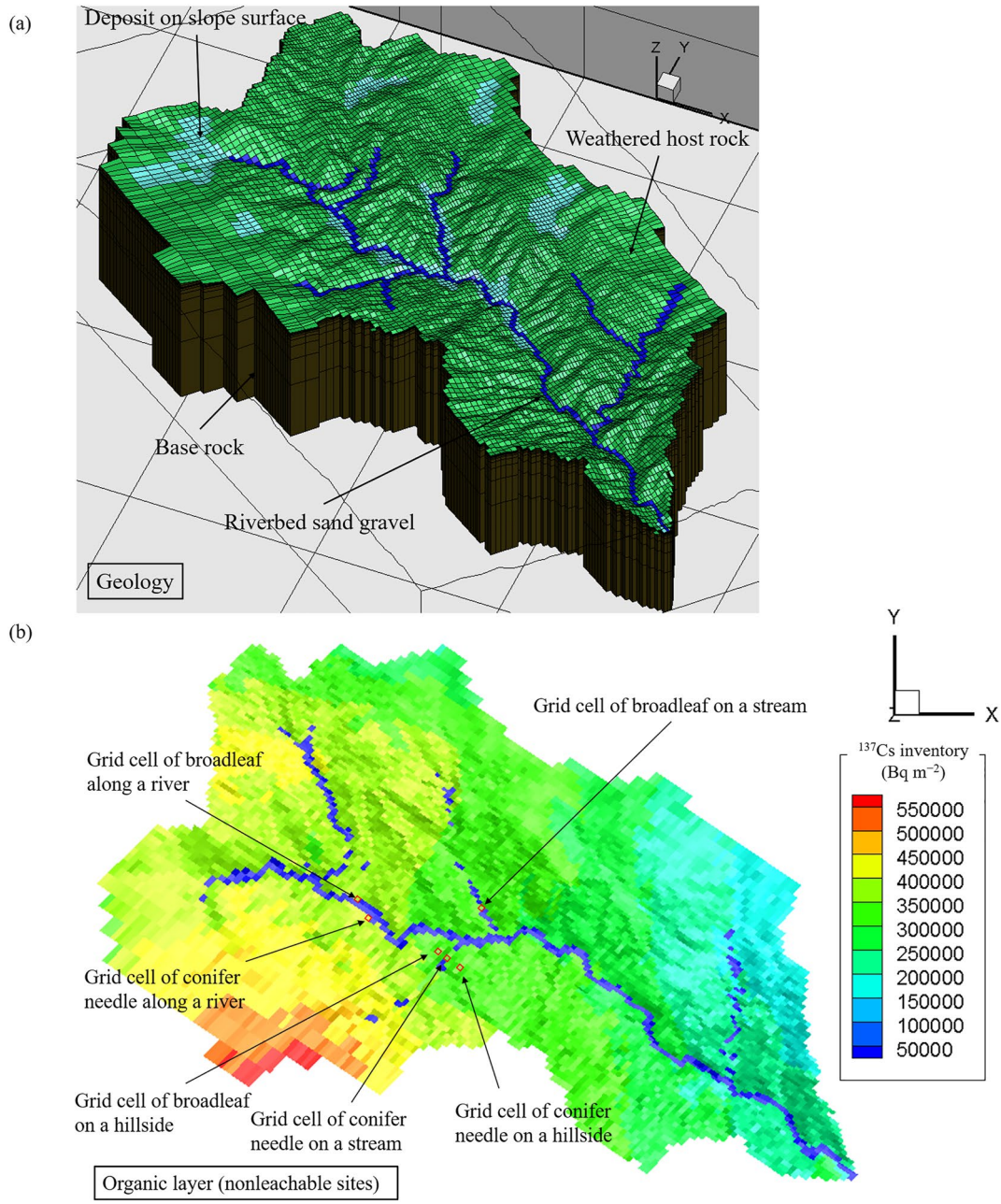

Figure 3. (a) The study area's 3D hydrogeological structure model. The colors indicate different deposits and bedrock types (individually labeled). (b) ^{137}C inventory in the organic layer (nonleachable sites) in the initial state of simulation Case 3. The red squares show grid cells on a stream, along a river, and on a hillside for each forest ecosystem compartment model monitored in Figure 7.

from air dose rates are provided in Sakuma, Tsuji, et al. (2018). Constant ^{137}Cs radioactivity concentrations, down to a depth of 2 cm below the surface and zero radioactivity in the soil beneath were assumed for the radioactivity distribution within the ground. A 2-cm thick radioactive topsoil layer was chosen because measurements have shown that ^{137}Cs remain in the upper soil near the ground surface (Takada et al., 2017; Yoschenko et al., 2017). The initial ^{137}Cs activity in the cells, covered by more than 2 cm of surface water after a spin-up simulation, was zero as the initial condition. An activity density per unit area (Bq m^{-2}) was assigned for each cell, based on the nearest airborne monitoring survey datum.

Table 1
Parameters for Forest Ecosystem Compartment Model

Pathway	Symbol	Unit	Conifer needle	Broadleaf	Reference
Tree external → Tree internal	k_1	s^{-1}	0	0	Hashimoto et al. (2013)
Tree internal → Organic layer (nonleachable sites)	k_2	s^{-1}	1.22×10^{-8}	7.57×10^{-9}	Hashimoto et al. (2013)
Soil → Tree internal	k_3	s^{-1}	5.17×10^{-10}	4.10×10^{-10}	Hashimoto et al. (2013)
Tree external → Organic layer (nonleachable sites)	k_4	s^{-1}	3.25×10^{-8}	3.54×10^{-8}	Hashimoto et al. (2013)
Organic layer (nonleachable sites) →Organic layer (leachable sites)	k_5	$A\ s^{-1}$	3.17×10^{-9}	3.17×10^{-9}	Tuned one-tenth times lower based on Kawahara (1985), with reference to Sakuma et al. (2021)
		B –	−1.66	−1.66	Kawahara (1985)
		$C\ °C^{-1}$	6.38×10^{-2}	9.57×10^{-2}	Tuned 1.5 times higher for broadleaves based on Kawahara (1985) with reference to Kurikami et al. (2019)
Organic layer (leachable sites) → Soil	k_6	s^{-1}	1.20×10^{-8}	1.87×10^{-8}	Kurikami et al. (2019)
Organic layer (leachable sites) → Surface water	k_7	s^{-1}	8.55×10^{-6}	4.81×10^{-5}	Kurihara et al. (2020)
Threshold water depth		m	0.005	0.005	Assumed
Soil → Organic layer (nonleachable sites)	k_8	s^{-1}	5.39×10^{-10}	1.17×10^{-9}	Kurihara et al. (2018)
Organic layer (nonleachable sites) → Soil	k_9	s^{-1}	1.20×10^{-8}	1.87×10^{-8}	Kurikami et al. (2019)

The setup of the forest compartment model was as follows. Table 1 shows the model's parameters. Kinetic rates k_1–k_4 were set based on Hashimoto et al. (2013). The rate k_5, that is, parameters A, B, and C, were set based on Kawahara (1985). These parameters were calculated from the weight loss of forest litter in a litterbag experiment on the forest floor. Because the weight loss of forest litter and ^{137}Cs transfer from nonleachable to leachable sites in the organic layer differs between forest types, parameters A of k_5 were calibrated based on ^{137}Cs leaching experiments (Sakuma et al., 2021). Consequently, parameter A of k_5 for conifer needle and broadleaves was set 10 times lower than Kawahara (1985). Also, parameter C of k_5 for broadleaves was 1.5 times higher than for conifer needles, referring to Kurikami et al. (2019) (from Table 1, parameter k_9 for broadleaves and conifer needles are 1.87×10^{-8} and 1.20×10^{-8}, respectively; therefore, $1.87 \times 10^{-8}/1.20 \times 10^{-8} \approx 1.5$). The parameter C value used in this study for broadleaf trees correlated with the results of Sakuma et al. (2021), showing that ^{137}Cs leaches more readily from broadleaf litter than conifer needle litter. Parameters k_6 and k_9 describing the transfer from the organic layer (leachable and non-leachable sites) to surface soil were set based on the study by Kurikami et al. (2019). Kurikami et al. (2019) estimated the transfer rates between forest compartments by inverse fitting analysis and applied the compartment model to two Sugi cedar forest sites, a hinoki cypress forest site, and a konara oak forest site. Therefore, the mean transfer rates from the litter layer to soil at three sites of Sugi cedar and hinoki cypress and the transfer rate at the konara oak forest site were used in this model. Parameter k_7 for the transfer from leachable sites in the organic layer to surface water was set based on Kurihara et al. (2020). Kurihara et al. (2020) conducted a serial ^{137}Cs leaching test from forest litter obtained from Japanese cedar and deciduous broadleaf forests and measured cumulative ^{137}Cs leachable fractions. The leachate was separated six times after 0.5, 7.5, 15, 30, 60, and 120 hr during the 5-day (120 hr) leaching test. We calculated the transfer rates from leachable sites in the litter to water under soaking conditions using the leaching results for recently fallen leaves of Japanese cedar and relatively old but unfragmented leaves of broadleaf, assuming that most ^{137}Cs in the leachable site are leached during 120 hr. The parameter k_8 for the transfer from surface soil to non-leachable sites in the organic layer was set based on the study by Kurihara et al. (2018).

Table 2
The Proportion of ^{137}Cs Activity in Each Media as Initial Condition of the Simulation

Tree type	Tree external	Tree internal	Organic layer (nonleachable sites)	Organic layer (leachable sites)	Surface soil
Conifer needle[a]	0.07	0	0.2	0	0.73
Broadleaves[a]	0.02	0	0.2	0	0.78

[a]Imamura et al. (2017).

Table 2 shows the division of the initial ^{137}Cs inventory between the forest canopy, the organic layer, and surface soil. These values were estimated based on Imamura et al. (2017). The simulation period was during 2014–2015; therefore, the measurements from August–September 2013 and 2014 were used to estimate the initial condition on 1 January 2014. The proportion

Table 3
Setup of Each Simulation Case

Simulation case	Forest ecosystem compartment model	Kinetics [s^{-1}]	Distribution coefficient (K_d) [$m^3\ kg^{-1}$]
Case 0	×	1.2[a]	200 (0.001–0.01 mm)
			50 (0.1–0.3 mm)
Case 1	×	1.0×10^{-6} (sorption)[b]	200 (0.001–0.01 mm) [c]
		1.0×10^{-8} (desorption)[b]	50 (0.1–0.3 mm) [c]
Case 2	×	1.0×10^{-6} (sorption)	360 (0.001–0.01 mm) [d]
		1.0×10^{-8} (desorption)	50 (0.1–0.3 mm)
Case 3	○	1.0×10^{-6} (sorption)	360 (0.001–0.01 mm)
		1.0×10^{-8} (desorption)	50 (0.1–0.3 mm)

[a]Instantaneous equilibrium was assumed. [b]Kurikami et al. (2017). [c]Sakuma, Tsuji, et al. (2018). [d]Tsuji et al. (2016).

of ^{137}Cs activity in tree internal in the initial state was set to zero because Imamura et al. (2017) reported that the ^{137}Cs inventory in wood accounted for less than 1% of the total at all plots, except for one site (<2%) in 2015. Also, Figure 3 (b) shows the ^{137}Cs distribution in non-leachable sites in the organic layer at the initial state based on these results.

The solid–liquid partitioning of the ^{137}Cs inventory was modeled with distribution coefficients $K_{d,i}$, where i denotes different particle sizes. GETFLOWS models six particle sizes with representative diameters of 0.001, 0.01, 0.1, 0.3, 1, and 5 mm. The distribution coefficients were set at 0 $m^3\ kg^{-1}$ for the 1 and 5-mm diameter sizes because of the low affinity for large particles to bind ^{137}Cs (He & Walling, 1996; Livens & Baxter, 1988). The distribution coefficients for the 0.001- and 0.01-mm sizes were set at 200–360 $m^3\ kg^{-1}$. These were based on the partitioning between dissolved ^{137}Cs and bound ^{137}Cs in suspended solids measured from river water samples collected at the catchment outflow during 2014–2015 ($361 \pm 242\ m^3\ kg^{-1}$, $n = 33$ under baseflow conditions, and $197 \pm 77\ m^3\ kg^{-1}$, $n = 24$ during three typhoons on 6 October 2014, 14 October 2014, and 16 July 2015) by Tsuji et al. (2016) and Sakuma, Tsuji, et al. (2018). The distribution coefficients for the 0.1- and 0.3-mm sizes were set to 50 $m^3\ kg^{-1}$ based on the study by Sakuma, Tsuji, et al. (2018).

To obtain a steady-state of the water and sediment flows over the catchment, that is, obtaining average surface and subsurface water and sediment flows in the fields, we performed a long-time equilibration simulation (water: approximately 6.0×10^7 days, sediment: approximately 6.0×10^4 days) using annual average precipitation and evapotranspiration values. The annual average precipitation (3.67 mm day^{-1}) and potential evapotranspiration (1.34 mm day^{-1}) were calculated using weather data from the Haramachi (1976–2015) and Namie (1981–2010) weather stations (Japan Meteorological Agency, 2015) using the Hamon method (Hamon, 1961).

Table 3 summarizes the setup of each simulation case reported in Section 3. Sakuma, Tsuji, et al. (2018) reported simulation Case 0. In this study, simulation Case 3 was conducted using the new coupled watershed-geochemical model. Simulation Case 3 differed in three ways from simulation Case 0. (a) The coupling of the organic layer described in the forest ecosystem compartment model allowed ^{137}Cs leaching from organic matter to rivers. (b) It considered the kinetics of adsorption and desorption at equilibrium between solid and aqueous phases based on the distribution coefficient (K_d), rather than assuming instantaneous partitioning between the phases. (c) The K_d values of clay and silt were changed to lie in the range of the measured values (from 200 $m^3\ kg^{-1}$ in Case 0–360 $m^3\ kg^{-1}$ in Case 3). This was necessary because the new pathway was added for ^{137}Cs leaching from the organic matter, which added to river water dissolved ^{137}Cs levels. To reveal the effect of coupling the forest compartment model, simulation cases 1 and 2 were conducted to isolate the effects of changes (b) and c) before introducing the forest compartment model.

Simulation cases 1–3 covered 1 January 2014, to 31 December 2015, matching Sakuma, Tsuji, et al. (2018). Weather data for simulations, such as hourly rainfall, air temperature, sunshine duration, average wind velocity, and relative humidity, were measured near the catchment center and at the Iitate, Haramachi, and Fukushima weather stations (Japan Meteorological Agency, 2015). Further information is provided in Sakuma, Tsuji, et al. (2018).

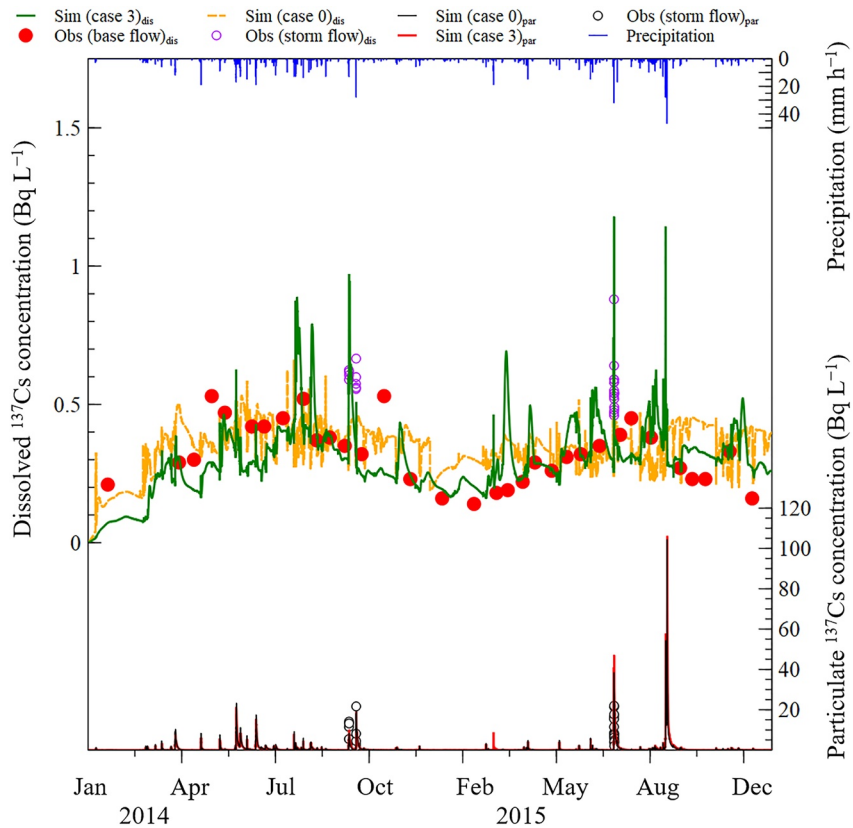

Figure 4. Simulation cases 0 and 3 and observation results for dissolved and particulate ^{137}Cs concentrations in river water at the catchment outflow point. Sim and Obs indicate simulated and observed ^{137}Cs concentrations, respectively. The suffix dis and par show dissolved and particulate ^{137}Cs concentrations, respectively.

We simulated water and suspended sediment discharge using the same initial and boundary conditions and input data as Sakuma, Tsuji, et al. (2018). Therefore, simulation cases 0–3 all gave identical results for water and suspended sediment discharge (Figures S1–S3, and cf. results in figures 3–5 of Sakuma, Tsuji, et al. (2018)).

2.5. Field Investigation

Tsuji et al. (2016) and Sakuma, Tsuji, et al. (2018) reported water discharge rates ($m^3\ s^{-1}$), suspended sediment fluxes ($kg\ s^{-1}$), and particulate and dissolved ^{137}Cs concentrations ($Bq\ L^{-1}$) during 2014–2015, including typhoon periods, at the catchment's outlet (Figure 1). We used these observed values as comparators for the simulation results of this study. From Tsuji et al. (2016), we considered baseflow conditions to be when water discharge rates were lower than 1.0 $m^3\ s^{-1}$. Detailed information on the field monitoring data was provided in Tsuji et al. (2016).

3. Results and Discussion

3.1. Comparison of Dissolved ^{137}Cs Concentrations in River Water Between Simulations With and Without the Forest Ecosystem Compartment Model

Figure S4 shows the results of simulation cases 1 and 2. This graph shows that modeling dissolved ^{137}Cs concentrations in river water based on K_d and/or kinetics changes cannot reproduce the observed trends. Figure 4 shows the results of simulation Case 3 with the coupled forest compartment model (green line) compared to Case 0 without the forest compartment model (orange line, Sakuma, Tsuji, et al., 2018). Modeling ^{137}Cs absorption and desorption between the dissolved and bound states with distribution coefficients (K_d) could not reproduce the seasonal variability in the baseflow dissolved ^{137}Cs concentrations and concentration peaks occurring during storms (Sakuma, Tsuji, et al., 2018). In the coupled model simulation (Case 3), higher temperatures in summer

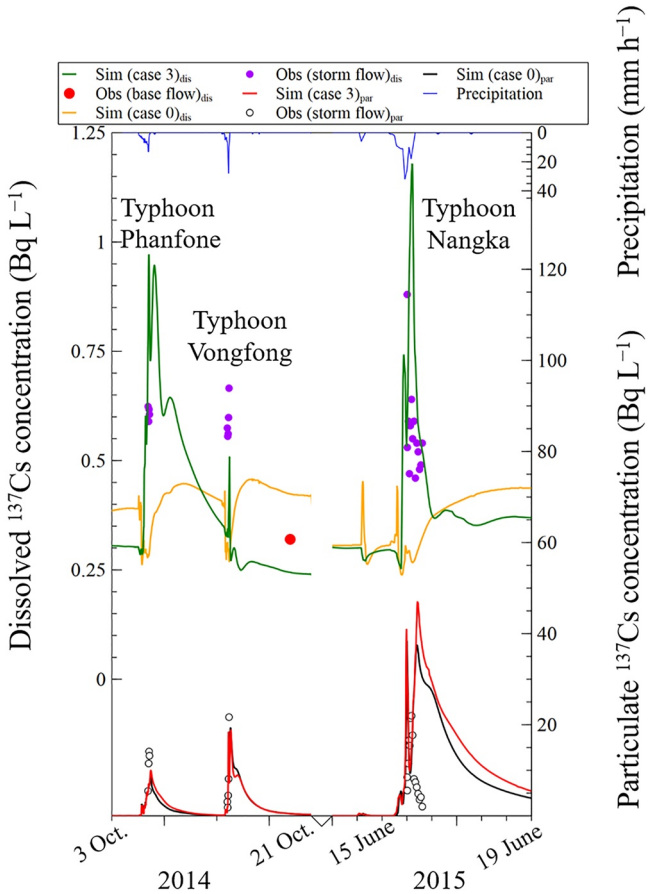

Figure 5. Simulation cases 0 and 3 and observation results for dissolved ^{137}Cs concentrations in river water under stormflow conditions at the catchment outflow point.

accelerate the ^{137}Cs transfer from the non-leachable Cs site to the leachable Cs site in the organic layer, functioning as a source of dissolved ^{137}Cs input to river water. Consequently, this model can reproduce the seasonal variability of baseflow dissolved ^{137}Cs concentrations. Although some of the observed baseflow dissolved ^{137}Cs concentrations are higher than the yearly trend, for example, red dots for May and November 2014, Figure 4, one possible factor is affected by the previous rainfall runoff (e.g., if there is flow in the area i.e., usually dry, this can be a source of the dissolved ^{137}Cs input to river water). However, the model has a structure that can reproduce dissolved ^{137}Cs concentrations in river water in a way that takes such effects into account, and as a result, accurately reproduces changes in concentrations during baseflow conditions.

The coupled simulation model can also reproduce the tendency of dissolved ^{137}Cs concentration increases and decrease, in line with the volume of water discharged, during storms. The simulations without the forest compartment model (Case 0) cannot do this well (Figure 5, Sakuma, Tsuji, et al., 2018). In the simulation results for the two consecutive typhoons in 2014, the spike in dissolved ^{137}Cs concentrations is smaller in the second storm than in the first storm. Possible reasons for this are the simulated water discharged rates at peaks in the second storm were underestimated by approximately 30% (Figure S3 in Supporting Information S1, refer to the result in figure 5 of Sakuma, Tsuji, et al. [2018]), showing that the riparian zone that submerged during storms in the simulation was smaller than reality. Additionally, the simulation grid cell resolution (approximately 40 m) is large compared to the width of mountain streams (approximately 1–5 m). Therefore, underestimates or overestimates of ^{137}Cs leaching from the organic layer might occur because the grid cell size affects the surface runoff area. Moreover, because we used forest compartment model parameters from the literature, using site-specific parameters may improve the correspondence of the simulation results with the observations.

Figure 6 shows the correlation between the observed and simulated results with and without the forest compartment model. For the results from Sakuma, Tsuji, et al. (2018) without the coupled forest compartment model, 91% of the results are within a factor of two of the measurements. The corresponding result with the forest compartment model is 93%, that is, slightly higher in this study than the Sakuma, Tsuji, et al. (2018) study. Furthermore, the Pearson correlation coefficient (r) is much better in this study ($r = 0.62$) than in the previous study ($r = -0.33$). The Pearson correlation coefficient is negative for the Case 0 simulation without the forest compartment model; therefore, the simulation results without the forest compartment model are only close to the observation results in magnitude but do not reproduce the dynamics of the two phenomena in the field. However, the Pearson correlation coefficient is positive for Case 3 with the forest compartment model; therefore, this model can better reproduce the dynamics of field observations. Furthermore, the root mean square error (RMSE) in Case 3 is slightly lower than Sakuma, Tsuji, et al. (2018) (RMSE = 0.214 in Case 3, and 0.216 in Case 0).

The results show that the Case 3 simulation could reproduce the seasonal variability in baseflow conditions and the peaks occurring during storms by modeling ^{137}Cs leaching from the organic layer in forests. This supports the theory that the organic layer in forests contributes significantly to contaminating the river water and the ecosystem in this catchment.

3.2. Temporal Changes in the Relative ^{137}Cs Inventory in Each Forest Compartment

Figure 7 shows the results for temporal changes in the relative ^{137}Cs inventory in each forest compartment at six representative grid cells within the catchment (on a stream, along a river, and on a hillside) (Figure 3 (b)). The relative ^{137}Cs inventory is the temporal change for each compartment divided by the total initial ^{137}Cs inventory in each grid cell. Comparing the simulated and measured values, the simulation underestimates the decrease rate

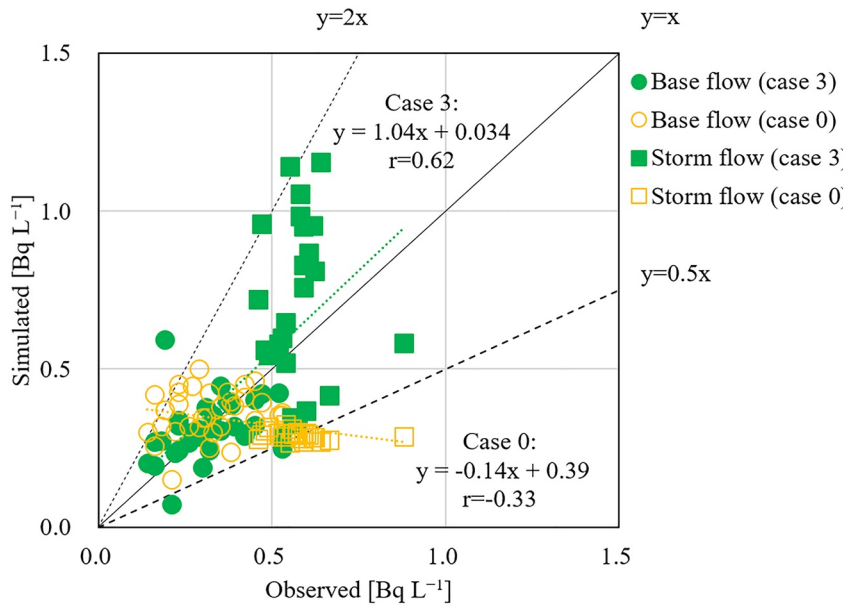

Figure 6. A scatter plot of observed and simulated dissolved ^{137}Cs concentrations at the catchment outflow under baseflow conditions ($n = 57$).

in the relative ^{137}Cs inventory of conferring needle litter. However, the relative ^{137}Cs inventory of the litter is roughly reproduced for the broadleaf compartment. The increase rate of the relative ^{137}Cs inventory of the tree internal compartments for broadleaf trees is also overestimated. However, this quantity is better reproduced for conifer needle trees. Furthermore, the decrease rate in the relative ^{137}Cs inventory of tree external for broadleaves is underestimated but can be roughly reproduced in conifer needle trees.

Overall, temporal changes in the ^{137}Cs inventory of litter, the key component supplying ^{137}Cs to the river, were reproduced well. In Figure 7 (a) and (b), litter decomposition depending on the temperature affects the simulation results for the ^{137}Cs inventory of leachable sites in the litter at grid cells on a stream. The relative ^{137}Cs inventory in the broadleaf compartment is approximately one order of magnitude lower than in the conifer needle compartment because ^{137}Cs can leach into the river water from the broadleaf litter at a higher rate. From Figure 7 (c) and (d), leachable ^{137}Cs in the litter at grid cells along a river can provide dissolved ^{137}Cs to the river under stormflow conditions from the stock in this model. The broadleaf compartment especially depletes the stock under stormflow conditions due to the high transfer rate from litter to water. However, conifer needle stock depletion occurs only under heavy stormflow conditions due to the low transfer rate from litter to water. That is, heavier stormflow conditions can make the duration of surface water runoff in this model longer, causing ^{137}Cs leaching from the conifer needle, even if there is a low transfer rate from litter to water. Also, the relative ^{137}Cs inventory of leachable sites in the conifer needle and broadleaf litter during simulation periods from 2014 to 2015 increased by approximately 0.3% and 0.1% in maximum, respectively. Therefore, the stock of leachable sites in the litter was 1.5%–3.0% and 0.5%–1%, respectively, considering that the relative ^{137}Cs inventory in the litter is approximately 0.1–0.2 during the simulation periods.

Manaka et al. (2019) reported that the proportion of exchangeable ^{137}Cs in organic layer samples significantly decreased within 2–4 years after the accident, becoming almost constant (2%–4%). Also, Sakuma et al. (2021) reported that after soaking conifer needle and broadleaf litter for 20 min, 140 min, and 1 day, the ^{137}Cs leaching ratio mean values were 0.13%–2.0% and 0.81%–6.6%, respectively, implying that the ^{137}Cs stock of leachable sites in the litter in this model correlates with the ^{137}Cs leaching experiments. Thus, the simulation results from 2014 to 2015 are reasonable. From Figure 7 (e) and (f), the relative ^{137}Cs inventory of leachable sites in the litter for conifer needle and broadleaf at grid cells on a hillside reached approximately 1% (which is also 5%–10% of the total litter inventory) due to the equilibrium between the downward migration from the leachable site organic layer to the soil layer and litter decomposition (from the non-leachable site to the leachable site in the organic

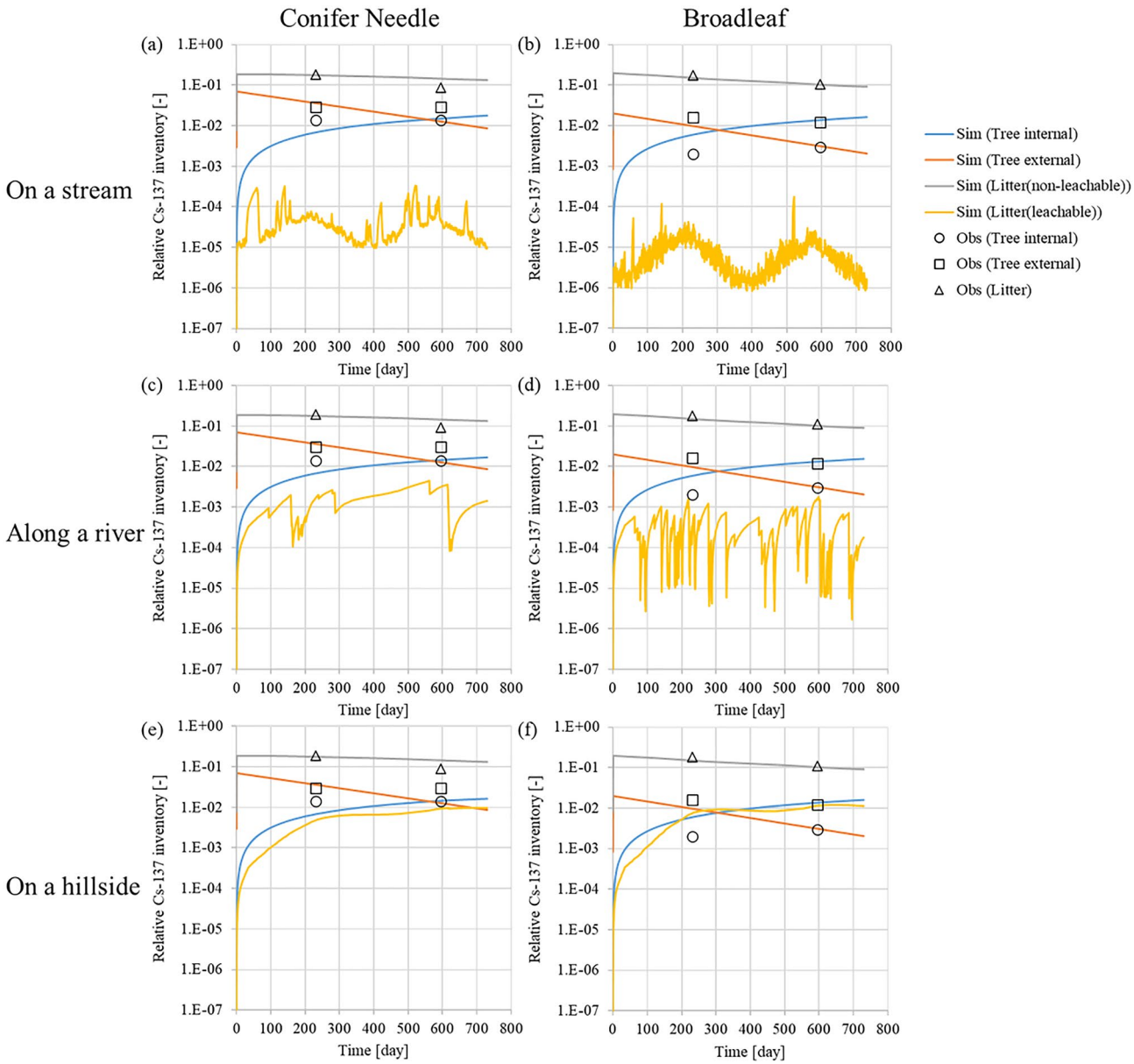

Figure 7. Simulation Case 3 and observation results for relative ^{137}Cs inventory for each forest ecosystem compartment model at cells on a stream, along a river, and on a hillside. Sim and Obs indicate simulated and observed relative ^{137}Cs inventory, respectively. The graph shows observations from Imamura et al. (2017). The left-hand side shows a conifer needle, and the right-hand side shows a broadleaf.

layer) in this model. This is because transfers from the leachable site in the litter to river water do not occur at grid cells located far from streams.

Because of this, Figure 7 (e) and (f) do not show short-term fluctuations in the relative ^{137}Cs inventory of the leachable site which occur for grid cells in the vicinity of streams (Figure 7 (a)–(d)). The model does not directly consider the process of ^{137}Cs leaching from litter by rainwater infiltration, which would also cause short-term fluctuations in the leachable fraction. Although the short-term dynamics are not captured, the average fraction of the leachable ^{137}Cs inventory across the year is comparable to measurements by Manaka et al. (2019) and Sakuma et al. (2021).

From Figure 7, the transfer trend from the tree and litter layer to the soil layer during 2014–2015 is also consistent with the simulation results reported by Hashimoto et al. (2021), describing that the relative ^{137}Cs inventory in the

surface soil layer increases gradually due to the downward migration from the organic layer to the surface soil layer.

3.3. Improvement of Reproducibility by Coupling the Forest Ecosystems Model With Watershed Modeling to Simulate Dissolved and Particulate ^{137}Cs Discharges

Coupling the forest ecosystem compartment model to reproduce the phenomenon of ^{137}Cs leaching from organic matter could improve the reproducibility of the concentration peaks occurring during typhoon events and seasonal variations under baseflow conditions. Sakuma, Tsuji, et al. (2018) discussed the limitations and applicability of the K_d theory, frequently used to explain dissolved ^{137}Cs concentrations in river water. This theory considers only absorption and desorption between dissolved and bound states. This study can reproduce phenomena seen in field observations by considering ^{137}Cs leaching from organic matter in addition to absorption and desorption between the dissolved and bound states. Although it is challenging simulating surface and subsurface water flows, sediment transport, and dissolved and particulate matter transport coupled with the compartment model, this study revealed it is necessary to consider leaching from organic materials in forest ecosystems when considering radioactive material discharge. From the perspective of bioavailability, understanding the dynamics of organically bound and dissolved radionuclides is vital when considering their transfer to wild creatures, for example, dissolved ^{137}Cs transfer from river water to freshwater fish. Many studies on watershed modeling (Kinouchi et al., 2015; Mori et al., 2015; Sakuma et al., 2017; Sakuma, Malim et al. 2018; Sakuma, Tsuji, et al. 2018; Wei et al., 2017) and the forest ecosystem compartment model (Calmon et al., 2015; Hashimoto et al., 2013; Kurikami et al., 2019; Nishina et al., 2018; Ota et al., 2016; Thiry et al., 2018) exist. However, watershed and forest compartment models have been developed independently because of different application scales and numerical approaches. This study revealed that we could better understand the phenomena of radioactive material discharges from catchments by integrating these models and modeling them against field data. This is true for ^{137}Cs discharges and discharges of other substances adsorbing onto surface soils and leaching from organic matter. Also, freshwater or coastal ecosystems are connected to forests. This study's modeling approach will be valuable in environmental radioactivity and local ecosystem assessment.

4. Conclusions

We developed a watershed-geochemical model by coupling a forest compartment model to GETFLOWS. The new model was used to simulate water, sediment, and ^{137}Cs (both dissolved and particulate-bound forms) in an upstream catchment of the Ohta River in the Fukushima Prefecture. The model reproduced the observed trends for dissolved ^{137}Cs concentrations in river water in base- and stormflow conditions. Overall, temporal changes in the ^{137}Cs inventory of forest compartments were also reproduced well. Modeling the dissolved ^{137}Cs concentrations in river water based only on desorption and resorption to bound states using distribution coefficients (K_d), could not reproduce the seasonal variability in baseflow conditions or the peaks occurring during storms (Sakuma, Tsuji, et al., 2018). The mechanisms captured in the new coupled model include the presence of easily soluble ^{137}Cs such as the leachable Cs site in the organic layer, the ^{137}Cs transfer from the non-leachable Cs site to the leachable Cs site in the organic layer depending on the bulk temperature, and the ^{137}Cs leaching kinetics on the hour-scale from the organic layer associated with water level fluctuations. The results are thus consistent with the theory that ^{137}Cs leaching from organic matter is an important contributor of dissolved ^{137}Cs to river water.

Seasonal variability of dissolved ^{137}Cs concentrations has also been reported in downstream areas of this and other catchments in Fukushima Prefecture, including outside forest areas (Nakanishi & Sakuma, 2019). Therefore, since such basins include various land uses, including fields, urban areas, and dam lakes, a possibility exists of seasonal variabilities in dissolved ^{137}Cs concentrations in river water due to the temperature dependence of the distribution coefficient, and not necessarily owing to litter decomposition. Furthermore, the increase in dissolved ^{137}Cs concentrations due to the increased area of flooded land could be reproduced, but the change in ^{137}Cs dynamics due to soil erosion might not be reproduced in this model. Also, modeling the behavior of particulate organic matter (POM) or litter (provided from the riparian zone and discharged due to the stormflow) in the river channels remains an open challenge because it is probable inputs of dissolved ^{137}Cs toward the river water originating from contaminated POM stored in riverine sediments themselves (Naulier et al., 2017).

This sedimentary could provide delayed source term of dissolved ^{137}Cs in river water because biodegradation is highly enhanced, especially in summer, in riverine sediments which consequently release dissolved contaminants. Further modeling improvements are needed in these areas in future.

The developed model should be valuable for planning decontamination strategies for forest management considerations and assessing water resources in contaminated regions after the nuclear accident. Similarly, the coupled watershed-geochemical model developed here could be used for simulating the transport of other substances in forest catchments where both particulate-bound and dissolved transfer mechanisms are important.

Conflict of Interest

The authors declare no conflicts of interest relevant to this study.

Data Availability Statement

Simulation results from this work can be obtained from Zenodo (https://doi.org/10.5281/zenodo.5861675).

Acknowledgments
We thank members of the Sector of Fukushima Research and Development and the Center for Computational Science & e-Systems for their support to this research. We also thank the staff at Geosphere Environmental Technology Corporation for their assistance on operating GETFLOWS.

References

Calmon, P., Gonze, M.-A., & Mourlon, C. (2015). Modeling the early-phase redistribution of radiocesium fallouts in an evergreen coniferous forest after Chernobyl and Fukushima accidents. *Science of the Total Environment*, *529*, 30–39. https://doi.org/10.1016/j.scitotenv.2015.04.084

Ewen, B. J., Parkin, G., & O'Connell, P. E. (2000). Shetran: Distributed river basin flow and transport modeling system. *Journal of Hydrologic Engineering*, *5*(3), 19233. https://doi.org/10.1061/(asce)1084-0699(2000)5:3(250)

Geological (2012). Survey of Japan. Retrieved from https://www.gsj.jp/en/index.html Accessed 9 March 2015.

Geospatial Information Authority of Japan. (2012). [Retrieved from Retrieved from http://www.gsi.go.jp/%20ENGLISH/ Accessed 9 March 2015.

Goderniaux, P., Brouyère, S., Fowler, H. J., Blenkinsop, S., Therrien, R., Orban, P., & Dassargues, A. (2009). Large scale surface-subsurface hydrological model to assess climate change impacts on groundwater reserves. *Journal of Hydrology*, *373*, 122–138. https://doi.org/10.1016/j.jhydrol.2009.04.017

Graham, D. N., & Butts, M. B. (2005). Flexible, integrated watershed modelling with MIKE SHE. In V. P. Singh, & D. K. Frevert (Eds.), *Watershed models* (pp. 245–272). CRC Press.

Hamon, W. R. (1961). Estimating potential evapotranspiration. *Proceedings of the American Society of Civil Engineers*, *87*(HY 3), 107–120. https://doi.org/10.1061/jyceaj.0000599

Hashimoto, S., Matsuura, T., Nanko, K., Linkov, I., Shaw, G., & Kaneko, S. (2013). Predicted spatio-temporal dynamics of radiocesium deposited onto forests following the Fukushima nuclear accident. *Scientific Reports*, *3*, 2564. https://doi.org/10.1038/srep02564

Hashimoto, S., Tanaka, T., Komatsu, M., Gonze, M. A., Sakashita, W., & Kurikami, H. (2021). Dynamics of radiocaesium within forests in Fukushima—Results and analysis of a model inter-comparison. *Journal of Environmental Radioactivity*, *238–239*, 106721. https://doi.org/10.1016/j.jenvrad.2021.106721

He, Q., & Walling, D. E. (1996). Interpreting particle size effects in the adsorption of ^{137}Cs and unsupported ^{210}Pb by mineral soils and sediments. *Journal of Environmental Radioactivity*, *30*, 117–137. https://doi.org/10.1016/0265-931X(96)89275-7

Imamura, N., Komatsu, M., Ohashi, S., & Hashimoto, S. (2017). Temporal changes in the radiocesium distribution in forests over the five years after the Fukushima Daiichi Nuclear Power Plant accident. *Scientific Reports*, *7*, 8179. https://doi.org/10.1038/s41598-017-08261-x

Iwagami, S., Tsujimura, M., Onda, Y., Nishino, M., Konuma, R., Yamamoto, M., et al. (2017). Temporal changes in dissolved ^{137}Cs concentrations in groundwater and stream water in Fukushima after the Fukushima Dai-ichi Nuclear Power Plant accident. *Journal of Environmental Radioactivity*, *166*, 458–465. https://doi.org/10.1016/j.jenvrad.2015.03.025

Japan Meteorological Agency. (2015). Retrieved from http://www.jma.go.jp/jma/indexe.html Accessed 24 February 2016.

Japan Meteorological Agency. (2021). Retrieved from http://www.jma.go.jp/jma/indexe.html Accessed 3 December 2021.

Jones, J. P., Sudicky, E. A., & Mclaren, R. G. (2008). Application of a fully-integrated surface-subsurface flow model at the watershed-scale: A case study. *Water Resources Research*, *44*, 1–13. https://doi.org/10.1029/2006WR005603

Kawahara, T. (1985). *Carbon cycling in forest ecosystems: In reference to litter fall and its decomposition*. Rep. Bull. For. & for. Prod. Res. Inst. No. 334. Forestry and Forest Products Research Institute.

Kinouchi, T., Yoshimura, K., & Omata, T. (2015). Modeling radiocesium transport from a river catchment based on a physically-based distributed hydrological and sediment erosion model. *Journal of Environmental Radioactivity*, *139*, 407–415. https://doi.org/10.1016/j.jenvrad.2014.07.022

Kitamura, A., Kurikami, H., Sakuma, K., Malins, A., Okumura, M., Machida, M., et al. (2016). Redistribution and export of contaminated sediment within eastern Fukushima Prefecture due to typhoon flooding. *Earth Surface Processes and Landforms*, *1726*, 1708–1726. https://doi.org/10.1002/esp.3944

Kollet, S. J., & Maxwell, R. M. (2008). Capturing the influence of groundwater dynamics on land surface processes using an integrated, distributed watershed model. *Water Resources Research*, *44*(2), 1–18. https://doi.org/10.1029/2007WR006004

Kurihara, M., Onda, Y., Kato, H., Lo, N., Yasutaka, T., & Coppin, F. (2018). Radiocesium migration in the litter layer of different forest types in, Japan. *Journal of Environmental Radioactivity*, *187*, 81–89. https://doi.org/10.1016/j.jenvrad.2018.01.027

Kurihara, M., Onda, Y., & Yasutaka, T. (2020). Radiocesium migration in the litter layer of different forest types in, Japan. *Journal of Environmental Radioactivity*, *223–224*, 106417. https://doi.org/10.1016/j.jenvrad.2020.106417

Kurikami, H., Funaki, H., Malins, A., Kitamura, A., & Onishi, Y. (2016). Numerical study of sediment and ^{137}Cs discharge out of reservoirs during various scale rainfall events. *Journal of Environmental Radioactivity*, *164*, 73–83. https://doi.org/10.1016/j.jenvrad.2016.07.004

Kurikami, H., Kitamura, A., Yokuda, S. T., & Onishi, Y. (2014). Sediment and ^{137}Cs behaviors in the Ogaki Dam Reservoir during a heavy rainfall event. *Journal of Environmental Radioactivity*, *137*, 10–17. https://doi.org/10.1016/j.jenvrad.2014.06.013

Kurikami, H., Malins, A., Takeishi, M., Saito, K., & Iijima, K. (2017). Coupling the advection-dispersion equation with fully kinetic reversible/irreversible sorption terms to model radiocesium soil profiles in Fukushima Prefecture. *Journal of Environmental Radioactivity*, *171*, 99–109. https://doi.org/10.1016/j.jenvrad.2017.01.026

Kurikami, H., Sakuma, K., Malins, A., Sasaki, Y., & Niizato, T. (2019). Numerical study of transport pathways of ^{137}Cs from forests to freshwater fish living in mountain streams in Fukushima, Japan. *Journal of Environmental Radioactivity*, *208–209*, 106005. https://doi.org/10.1016/j.jenvrad.2019.106005

Laflen, J. M., Lane, L. J., & Foster, G. R. (1991). WEPP: A new generation of erosion prediction technology. *Journal of Soil Water Conservation*, *46*(1), 34–38.

Livens, F. R., & Baxter, M. S. (1988). Particle size and radionuclide levels in some west Cumbrian soils. *Science of the Total Environment*, *70*, 1–17. https://doi.org/10.1016/0048-9697(88)90248-3

Malagó, A., Bouraoui, F., Vigiak, O., Grizzetti, B., & Pastori, M. (2017). Modelling water and nutrient fluxes in the Danube river basin with SWAT. *Science of the Total Environment*, *604*, 196–218. https://doi.org/10.1016/j.scitotenv.2017.05.242

Manaka, T., Imamura, N., Kaneko, S., Miura, S., Furusawa, H., & Kanasashi, T. (2019). Six-year trends in exchangeable radiocesium in Fukushima forest soils. *Journal of Environmental Radioactivity*, *203*, 84–92. https://doi.org/10.1016/j.jenvrad.2019.02.014

Ministry of Agricultural, forestry, and fisheries. (2012). [Retrieved from Retrieved from http://www.rinya.maff.go.jp/j/keikaku/genkyou/h24/1.html Accessed 28 August 2019.

Ministry of EducationCulture, & Sports, S. T. (2011). Results of the third airborne monitoring survey by MEXT. Retrieved from http://www.mext.go.jp/component/english/__icsFiles/afieldfile/2011/07/22/1304797_0708e.pdf Accessed 24 November 2016.

Ministry of the Environment (2012). Retrieved from, Accessed 28 August 2019 (in Japanese).] http://josen.env.go.jp/material/session/pdf/009/ref01.pdf

Ministry of the Environment (2016). Natural environmental information GIS. [Retrieved from http://www.biodic.go.jp/trialSystem/top_en.html Accessed 4 November 2016.

Morgan, R. P. C., Quinton, J. N., Smith, R. E., Govers, G., Poesen, J. W. A., Auerswald, K., et al. (1998). *The European soil erosion model (EUROSEM): Documentation and user Guide*. Silsoe College, Cranfield University. Retrieved from https://eprints.lancs.ac.uk/id/eprint/13189/1/user_v2.pdf

Mori, K., Tada, K., Tawara, Y., Ohno, K., Asami, M., Kosaka, K., & Tosaka, H. (2015). Integrated watershed modeling for simulation of spatiotemporal redistribution of post-fallout radionuclides: Application in radiocesium fate and transport processes derived from the Fukushima accidents. *Environmental Modelling & Software*, *72*, 126–146. https://doi.org/10.1016/j.envsoft.2015.06.012

Murakami, M., Ohte, N., Suzuki, T., Ishii, N., Igarashi, Y., & Tanoi, K. (2014). Biological proliferation of cesium-137 through the detrital food chain in a forest ecosystem in Japan. *Scientific Reports*, *4*, 3599. https://doi.org/10.1038/srep03599

Muto, K., Andoh, M. A., Koarashi, J., Takeuchi, E., Nishimura, S., Tsuduki, K., & Matsunaga, T. (2017). Sources of ^{137}Cs fluvial export from a forest catchment evaluated by stable carbon and nitrogen isotopic characterization of organic matter. *Journal of Radioanalytical and Nuclear Chemistry*. https://doi.org/10.1007/s10967-017-5350-7

Nakanishi, T., Funaki, H., & Sakuma, K. (2021). Factors affecting ^{137}Cs concentrations in river water under base-fow conditions near the Fukushima Dai-ichi Nuclear Power Plant. *Journal of Radioanalytical and Nuclear Chemistry*, *328*, 1243–1251. https://doi.org/10.1007/s10967-021-07735-7

Nakanishi, T., & Sakuma, K. (2019). Trend of ^{137}Cs concentration in river water in the medium term and future following the Fukushima nuclear accident. *Chemosphere*, *215*, 272–279. https://doi.org/10.1016/j.chemosphere.2018.10.017

National Agriculture and Food Research Organization. (2021). [Available at(in Japanese) Retrieved from https://soil-inventory.dc.affrc.go.jp/kokusai.html Accessed 26 November 2021.

National Institute of Advanced Science and Technology. (2016). GeomapNavi. Retrieved from https://gbank.gsj.jp/geonavi/?lang=en Accessed 14 November 2017.

Naulier, M., Eyrolle-Boyer, F., Boyer, P., Métivier, J. M., & Onda, Y. (2017). Particulate organic matter in rivers of Fukushima: An unexpected carrier phase for radiocesiums. *Science of the Total Environment*, *579*, 1560–1571. https://doi.org/10.1016/j.scitotenv.2016.11.165

Nishina, K., Hashimoto, S., Imamura, N., Ohashi, S., Komatsu, M., Kaneko, S., & Hayashi, S. (2018). Calibration of forest ^{137}Cs cycling model "FoRothCs" via approximate Bayesian computation based on 6-year observations from plantation forests in Fukushima. *Journal of Environmental Radioactivity*, *193*, 82–90. https://doi.org/10.1016/j.jenvrad.2018.09.002

Nuclear Regulation Authority (2013). Retrieved from https://radioactivity.nsr.go.jp/ja/list/362/list-1.html, Accessed 24 February 2021 (in Japanese).]

Onishi, Y., Graber, H. C., & Trent, D. S. (1993). Preliminary modeling of wave-enhanced sediment and contaminant transport in New Bedford Harbor. In A. J. Mehta (Ed.), *Coastal and Estuarine studies* (Vol. 42). American Geophysical Union. https://doi.org/10.1029/ce042p0541

Onishi, Y., & Yokuda, S. T. (2013). *Simulate and evaluate the cesium transport and accumulation in Fukushima-area rivers by the TODAM code*. Rep. PNNL-22364). Pacific Northwest National Laboratory.

Ota, M., Nagai, H., & Koarashi, J. (2016). Modeling dynamics of ^{137}Cs in forest surface environments: Application to a contaminated forest site near Fukushima and assessment of potential impacts of soil organic matter interactions. *Science of The Total Environment*, *551*(552), 590–604. https://doi.org/10.1016/j.scitotenv.2016.02.068

Sakai, M., Gomi, T., & Negishi, J. N. (2016). Fallout volume and litter type affect ^{137}Cs concentration difference in litter between forest and stream environments. *Journal of Environmental Radioactivity*, *164*, 169–173. https://doi.org/10.1016/j.jenvrad.2016.07.030

Sakakibara, K., Iwagami, S., Tsujimura, M., Konuma, R., Sato, Y., & Onda, Y. (2021). Radiocesium leaching from litter during rainstorms in the Fukushima broadleaf forest. *Science of the Total Environment*, *796*. https://doi.org/10.1016/j.scitotenv.2021.148929

Sakuma, K., Kitamura, A., Malins, A., Kurikami, H., Machida, M., Mori, K., et al. (2017). Characteristics of radio-cesium transport and discharge between different basins near to the Fukushima Dai-ichi Nuclear Power Plant after heavy rainfall events. *Journal of Environmental Radioactivity*, *169–170*, 130–150. https://doi.org/10.1016/j.jenvrad.2016.12.006

Sakuma, K., Malins, A., Funaki, H., Kurikami, H., Niizato, T., Nakanishi, T., et al. (2018). Evaluation of sediment and ^{137}Cs redistribution in the Oginosawa River catchment near the Fukushima Dai-ichi Nuclear Power Plant using integrated watershed modeling. *Journal of Environmental Radioactivity*, *182*, 44–51. https://doi.org/10.1016/j.jenvrad.2017.11.021

Sakuma, K., Tsuji, H., Hayashi, S., Funaki, H., Malins, A., Yoshimura, K., et al. (2018). Applicability of K_d for modelling dissolved ^{137}Cs concentrations in Fukushima river water: Case study of the upstream Ota River. *Journal of Environmental Radioactivity*, *184*, 53–62. https://doi.org/10.1016/j.jenvrad.2018.09.013

Sakuma, K., Yoshimura, K., & Nakanishi, T. (2021). Leaching characteristics of ^{137}Cs for forest floor affected by the Fukushima nuclear accident: A litterbag experiment. *Chemosphere*, *264*, 128480. https://doi.org/10.1016/j.chemosphere.2020.128480

Santhi, C., Srinivasan, R., Arnold, J. G., & Williams, J. R. (2006). A modeling approach to evaluate the impacts of water quality management plans implemented in a watershed in Texas. *Environmental Modelling & Software*, *21*(8), 1141–1157. https://doi.org/10.1016/j.envsoft.2005.05.013

Shaw, G., Venter, A., Avila, R., Bergman, R., Bulgakov, A., Calmon, P., et al. (2005). Radionuclide migration in forest ecosystems - results of a model validation study. *Journal of Environmental Radioactivity*, *84*(2), 285–296. https://doi.org/10.1016/j.jenvrad.2003.09.006

Shinomiya, Y., Tamai, K., Kobayashi, M., Ohnuki, Y., Shimizu, T., Iida, S., et al. (2014). Radioactive cesium discharge in stream water from a small watershed in forested headwaters during a typhoon flood event. *Soil Science & Plant Nutrition*, *60*, 765–771. https://doi.org/10.1080/00380768.2014.949852

Siirila-woodburn, E. R., Steefel, C. I., Williams, K. H., & Birkholzer, J. T. (2018). Predicting the impact of land management decisions on overland flow generation: Implications for cesium migration in forested Fukushima watersheds. *Advances in Water Resources*, *113*, 42–54. https://doi.org/10.1016/j.advwatres.2018.01.008

Takada, M., Yamada, T., Takahara, T., Endo, S., Kajimoto, T., & Okuda, T. (2017). Temporal changes in vertical distribution of Cs in litter and soils in mixed deciduous forests in Fukushima, Japan. *Journal of Nuclear Science and Technology*, *54*(4), 452–458. https://doi.org/10.1080/00223131.2017.1287602

Thiry, Y., Albrecht, A., & Tanaka, T. (2018). Development and assessment of a simple ecological model (TRIPS) for forests contaminated by radiocesium fallout. *Journal of Environmental Radioactivity*, *190*, 149–159. https://doi.org/10.1016/j.jenvrad.2018.05.009

Tosaka, H., Kojima, K., Miki, A., & Chino, T. (1996). Numerical simulation of surface-subsurface-coupled, 2-phase, 3-dimensional fluid behavior. *Journal of Groundwater Hydrology*, *38*, 253–267. https://doi.org/10.5917/jagh1987.38.253

Tsuji, H., Nishikiori, T., Yasutaka, T., Watanabe, M., Ito, S., & Hayashi, S. (2016). Behavior of dissolved radiocesium in river water in a forested watershed in Fukushima Prefecture. *Journal of Geophysical Research: Biogeosciences*, *121*, 2588–2599. https://doi.org/10.1002/2016JG003428

Wei, L., Kinouchi, T., Yoshimura, K., & Velleux, M. L. (2017). Modeling watershed-scale ^{137}Cs transport in a forested catchment affected by the Fukushima Dai-ichi Nuclear Power Plant accident. *Journal of Environmental Radioactivity*, *171*, 21–33. https://doi.org/10.1016/j.jenvrad.2017.01.017

Yamada, S., Kurikami, H., & Machida, M. (2020). Applications of radiocesium migration models to Fukushima environmental Issues: Numerical analysis of radiocesium transport in temperature-stratified reservoirs by 3D-Sea-SPEC. *International conference on Supercomputing in nuclear applications + Monte Carlo 2020*. Paper presented at Joint(online).

Yoschenko, V., Takase, T., Konoplev, A., Nanba, K., Onda, Y., Kivva, S., et al. (2017). Radiocesium distribution and fluxes in the typical Cryptomeria japonica forest at the late stage after the accident at Fukushima Dai- Ichi Nuclear Power Plant. *Journal of Environmental Radioactivity*, *166*, 45–55. https://doi.org/10.1016/j.jenvrad.2016.02.017

Yoshikawa, N., Obara, H., Ogasa, M., Miyazu, S., Harada, N., & Nonaka, M. (2014). ^{137}Cs in irrigation water and its effect on paddy fields in Japan after the Fukushima nuclear accident. *Science of the Total Environment*, *481*(1), 252–259. https://doi.org/10.1016/j.scitotenv.2014.01.129

Zheleznyak, M. J. (1997). The mathematical modelling of radionuclide transport by surface water flow from the vicinity of the Chernobyl nuclear power plant. *Condensed Matter Physics*, *12*, 37–50. https://doi.org/10.5488/cmp.12.37

Water Resources Research

Supporting Information for

Watershed-geochemical model to simulate dissolved and particulate ^{137}Cs discharge from a forested catchment

Kazuyuki Sakuma[1*], Seiji Hayashi[2], Kazuya Yoshimura[1], Hiroshi Kurikami[1], Alex Malins[3], Hironori Funaki[1], Hideki Tsuji[2], Takamaru Kobayashi[4], Akihiro Kitamura[1], Kazuki Iijima[1]

[1] Sector of Fukushima Research and Development, Japan Atomic Energy Agency, Fukushima 963-7700, Japan.

[2] Fukushima Branch, National Institute of Environmental Studies, Fukushima 963-7700, Japan.

[3] Center for Computational Science & e-Systems, Japan Atomic Energy Agency, Chiba 277-0871, Japan.

[4] Geosphere Environmental Technology Corporation, Tokyo 101-0063, Japan.

Contents of this file

Introduction

Figure S1 shows simulated and observed water discharge rates from 2014 to 2015. Figure S2 shows simulated and observed suspended sediment fluxes between May 29, 2014, and Sep 10, 2015. Figure S3 shows simulated and observed water discharge rates and suspended sediment fluxes under stormflow conditions. Figure S4 shows the simulation results of cases 1 and 2.

The various input parameters used in these simulations are provided in Tables S1–S6. Table S1 lists Manning's roughness coefficient for land use and vegetation types. Table S2 lists raindrop-induced erosion parameters depending on the land use and vegetation type. Tables S3 and S4 list the hydraulic parameters for grid blocks in the surface soil and subsurface layers. These parameters were calibrated using hydrographs based on

observation data. Table S5 lists the sediment particle size distribution. We modeled six representative particle diameters of 0.001, 0.01, 0.1, 0.3, 1, and 5 mm, respectively. Although fine particle grades strongly adsorb ^{137}Cs, all grades affect ^{137}Cs concentrations so must be modeled. Table S6 lists soil detachment properties due to raindrops and surface water flow.

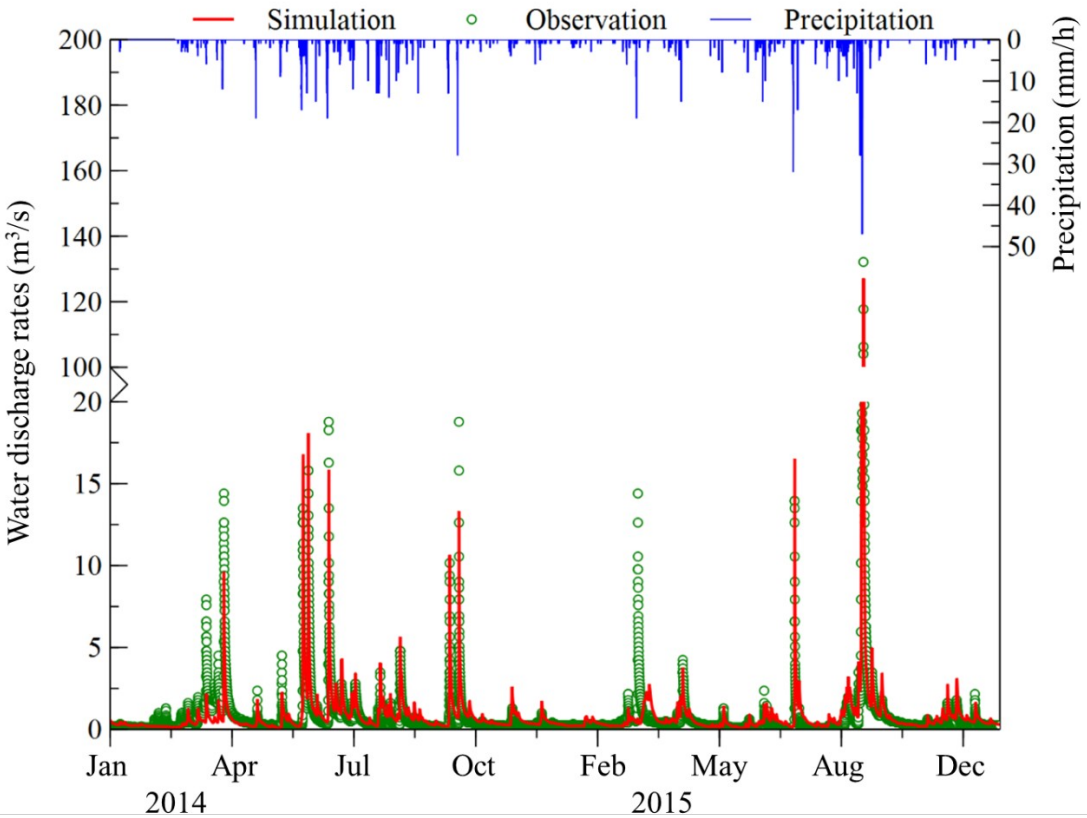

Figure S1. Simulated and measured hourly mean water discharge rates at the catchment outlet and hourly precipitation rates over the entire two-year study. Reprinted from the Journal of Environmental Radioactivity, 184–185, Sakuma et al., Applicability of K_d for modeling dissolved ^{137}Cs concentrations in Fukushima river water: Case study of the upstream Ota River, 53–62, Copyright (2018), with permission from Elsevier.

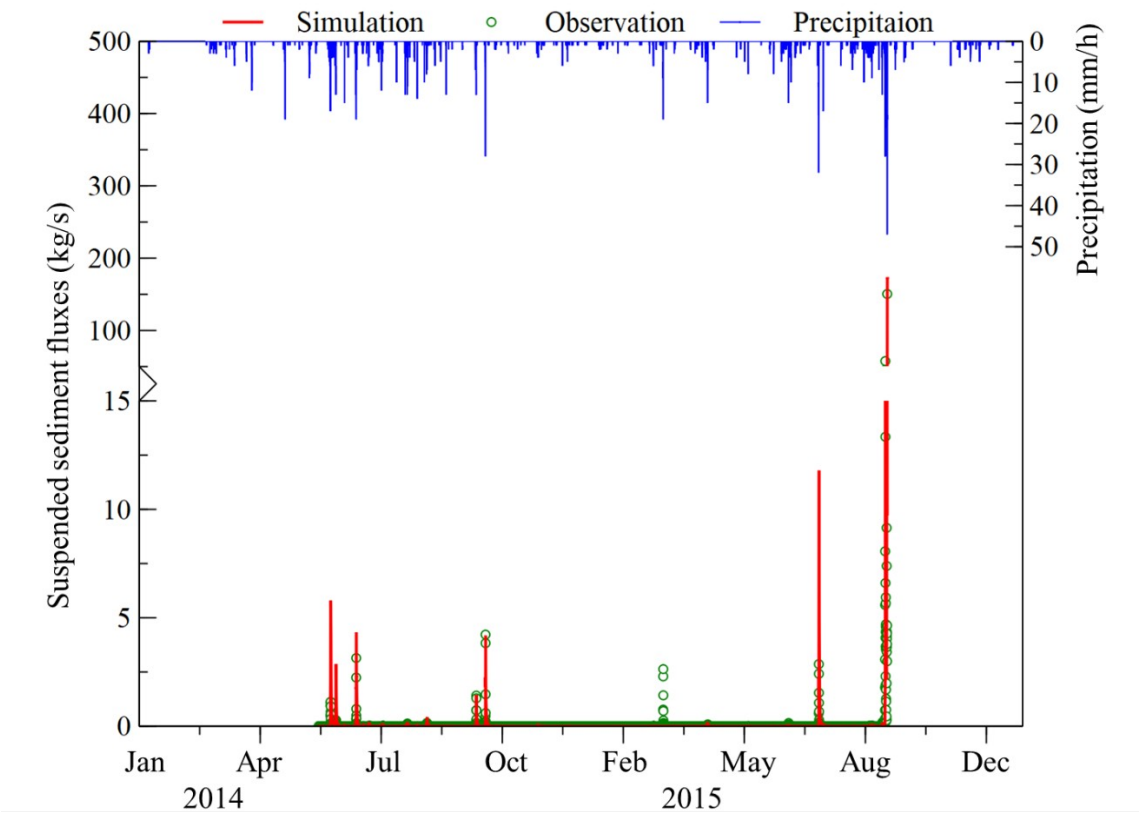

Figure S2. Simulated and measured hourly mean suspended sediment fluxes at the catchment outlet between May 29, 2014, and Sep 10, 2015. Reprinted from the Journal of Environmental Radioactivity, 184–185, Sakuma et al., Applicability of K_d for modeling dissolved ^{137}Cs concentrations in Fukushima river water: Case study of the upstream Ota River, 53–62, Copyright (2018), with permission from Elsevier.

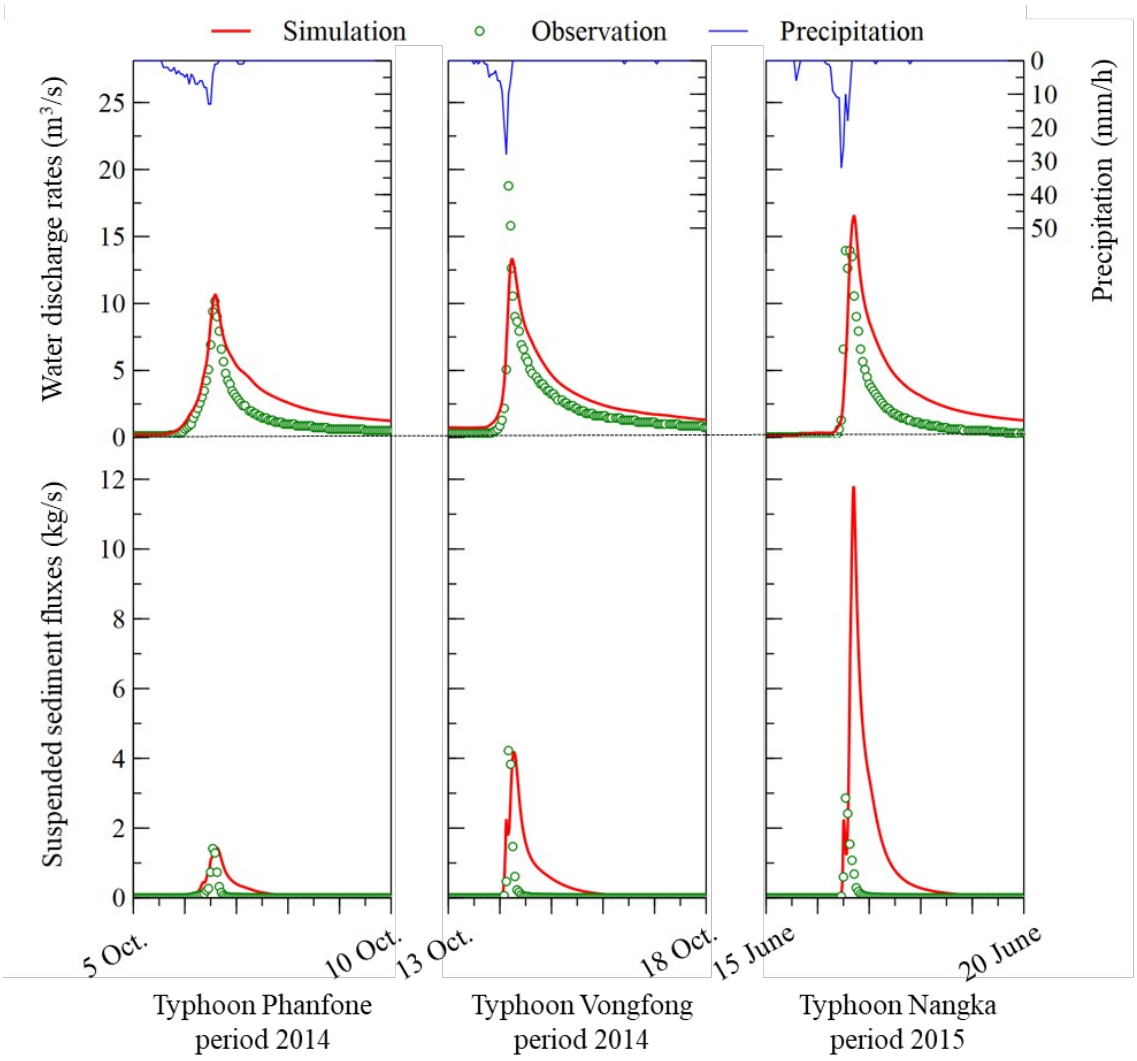

Figure S3. Simulated and measured river water discharge rates (upper panels) and suspended sediment fluxes (lower panels) at the catchment outlet during Typhoons Phanfone (October 5–10, 2014), Vongfong (October 13–18, 2014), and Nangka (June 15–20, 2015). The upper panels also show precipitation rates over the storms. Reprinted from the Journal of Environmental Radioactivity, 184–185, Sakuma et al., Applicability of K_d for modeling dissolved ^{137}Cs concentrations in Fukushima river water: Case study of the upstream Ota River, 53–62, Copyright (2018), with permission from Elsevier.

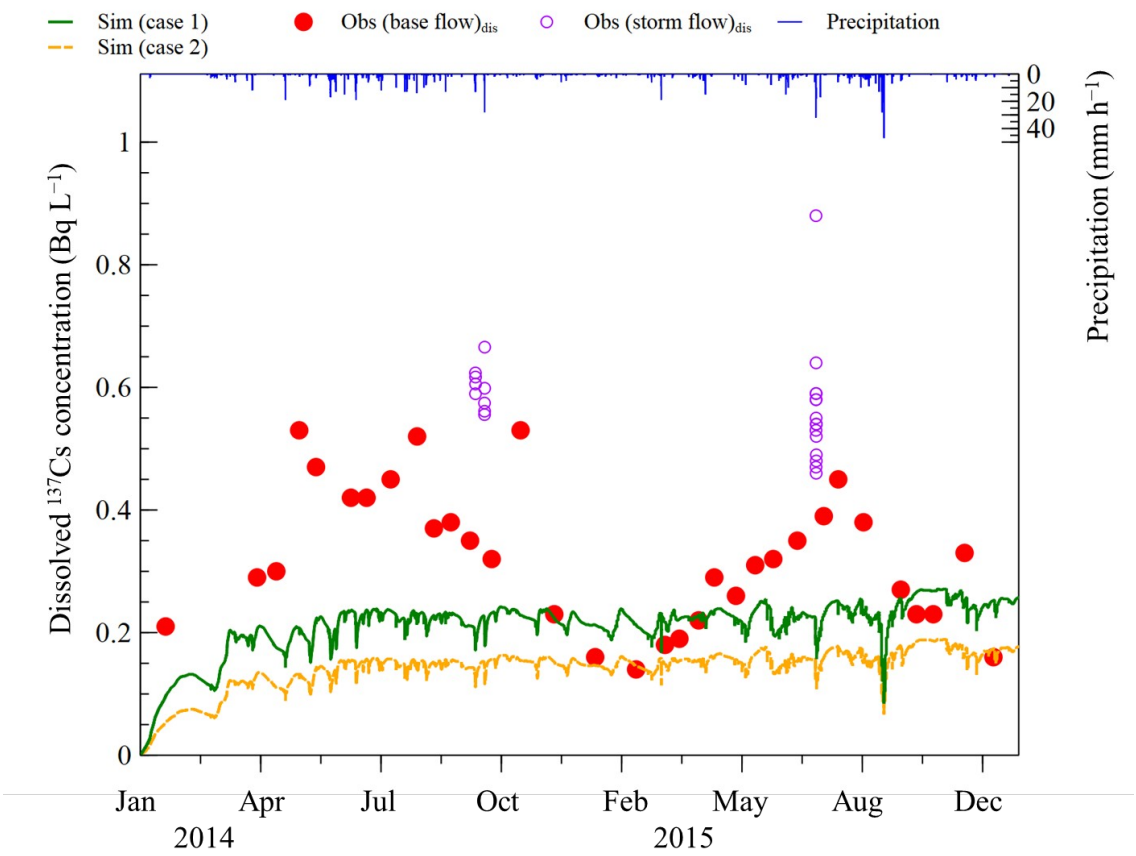

Figure S4. Simulation cases 1 and 2, and observation results for dissolved ^{137}Cs concentrations in river water at the catchment outflow point. Sim and Obs indicate simulated and observed ^{137}Cs concentrations, respectively. The suffix dis indicates dissolved ^{137}Cs concentrations.

Land use and vegetation type	Manning's roughness coefficient ($m^{-1/3}$ s)
Japanese cedar & cypress	0.5
Larch plantation	0.5
Deciduous broadleaf	0.8
River	0.03

Table S1. Manning's roughness coefficient for land use and vegetation types.

Land use and vegetation type	Canopy height (m)	Stem storage (mm)	Crown covering (—)	Floor storage (mm)	Floor covering (—)
Japanese cedar & cypress	15	1.5	0.8	0.25	0.95
Larch plantation	15	1.5	0.8	0.25	0.95
Deciduous broadleaf	15	1	0.8	0.25	0.95
River	0	0	0	0	0

Table S2. Raindrop-induced erosion parameters.

Soil	Land use	Subsurface	Intrinsic permeability ($m\ s^{-1}$)	Effective porosity (—)	Relative permeability and capillary curves
Forest brown soil	River	—	1×10^{-4}	0.7	Cohesive soil
	Forest	Weathered host rock	1×10^{-3}	0.5	Cohesive soil
		Deposit on slope surface	1×10^{-3}	0.5	Gravel soil
		Riverbed sand	1×10^{-3} (top 30 cm of surface soil)	0.5	Gravel soil
		Gravel	1×10^{-4} (soil between 30 cm and 100 cm)	0.4	Sandy soil

Table S3. Hydraulic parameters for grid blocks in the surface soil layers.

Geology	Intrinsic permeability (m s^{-1})	Effective porosity (—)
Riverbed sand gravel	1×10^{-4}	0.3
Deposits on slope surface	3×10^{-5}	0.3
Weathered host rock (west)	5×10^{-7} (horizontal) 1×10^{-8} (vertical)	0.2
Weathered host rock (east)	1×10^{-6} (horizontal) 1.5×10^{-7} (vertical)	0.2
Bedrock	1×10^{-8}	0.1

Table S4. Hydraulic parameters for grid blocks in the subsurface layers.

Soil	Land use	Subsurface	Sediment representative particle size (mm)					
			0.001	0.01	0.1	0.3	1	5
Forest brown soil	River	—	0.01	0.04	0.25	0.30	0.20	0.20
	Forest	Weathered host rock	0.03	0.42	0.15	0.2	0.1	0.1
		Deposit on slope surface	0.03	0.32	0.1	0.1	0.15	0.3
		Riverbed sand gravel	0.03	0.17	0.10	0.10	0.20	0.40

Table S5. Sediment particle size distribution.

Soil	Land use	Subsurface	SDI (g J^{-1})	Adhesion (kPa)
Forest brown soil	River	—	3.0	—
	Forest	Weathered host rock	50	10
		Deposit on slope surface	50	3
		Riverbed sand gravel	50	3

Table S6. Soil detachment properties.